Examining the Effect of Additional Driving Forces on a Mechanical Oscillator

Nate Stone
Physics Department, The College of Wooster, Wooster, Ohio 44691, USA
(Dated: May 7, 2015)

In this experiment, the motion of an oscillator similar to the Duffing oscillator was analyzed to determine how it varied from the original Duffing oscillator. In order to modify the oscillator, an additional motor was added onto the oscillator. The dual motor oscillator was then run at several different speeds, with different initial conditions. This was compared to the results obtained from the oscillator when the second motor was turned off. These tests were done, varying the multiple initial conditions, and the results were plotted in phase space plots, as well as Poincare plots. The vibrational motor prompted some interesting changes in the motion of the oscillator. There was a distinct pattern in the Poincare plots as the frequency of the second motor was increased. This pattern was something completely new, as previously there had been no correlation between frequency and motion. The rotary motor was also varied, while the vibrational motor stayed constant, however there was not a clear correlation between the motion and the frequency. Changing the amplitude of the rotary motor had the same effect on the motion of the oscillator as it did in the original Duffing oscillator. Once again there was no clear correlation between changing the amplitude of the driving force, and the motion of the system.

I. INTRODUCTION

Often, the motion of an oscillator follows a distinct pattern, with its future movements easily predicted. For example, take a simple pendulum, as shown in Fig. 1, whose motion is simply an oscillation between two arbitrary points. The motion of the pendulum is easily predicted, due to the fact that there will be no change in how the pendulum moves. This motion is described by the pendulum's equation of motion. An equation of motion is directly dependent on the kinetic and potential energies of the system. In order to derive the equation of motion from the kinetic and potential energies, the Lagrangian is used. The Lagrangian is a mathematical way of explaining the dynamics of a system. By using Lagrangian analysis, a differential equation, of varying order is obtained. This differential equation, when solved, results in the equation of motion. As stated earlier, this equation describes the motion of the system being studied, however there are cases where the equation of motion for a system does not accurately predict the motion of the system. This type of motion is said to be chaotic. Chaotic motion is a small piece of an overarching theory called Chaos Theory.

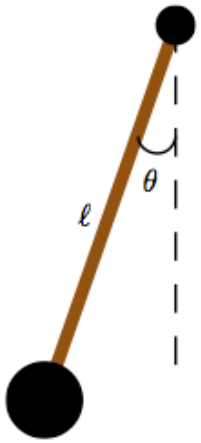

FIG. 1: The simple pendulum superimposed onto the Cartesian plane.[2]

Chaos Theory is a field of mathematics that focuses on dynamical systems, specifically ones that are very sensitive to initial conditions. The sensitivity to initial conditions is colloquially known as the butterfly effect. The butterfly effect states that a butterfly flapping its wings could manifest itself into a hurricane somewhere across the world.[1] This means that a slight change in a seemingly irrelevant factor drastically changes the overall system. Applying this idea to a mechanical oscillator, we see that a small change in one of the initial conditions of the oscillator will drastically change the motion. When a change is made to an initial condition, the motion of the oscillator can become chaotic. When a system's motion is said to be chaotic, there is no order to the system. This means that the motion of the system is completely randomized. Despite the fact that the motion of the system is random, some interesting phenomena occur.

In order to visualize some of these phenomena, a few different plots are used. First, a phase space plot, which is a plot of the angular velocity vs. the angular position, is used. The phase space plot shows how the oscillator is moving around its equilibrium points. Equilibrium points are positions that the oscillator can be at rest. There are two types of equilibrium, stable and unstable. A stable equilibrium point is a point that the oscillator will naturally fall into. An unstable equilibrium point is a point where the oscillator can be at rest, but will not naturally go to that point. For example, take a clock pendulum and imagine it swinging back and forth. If there is no added force, the pendulum will naturally hang straight down. This is the stable equilibrium point, because the oscillator can have almost any amount of en-

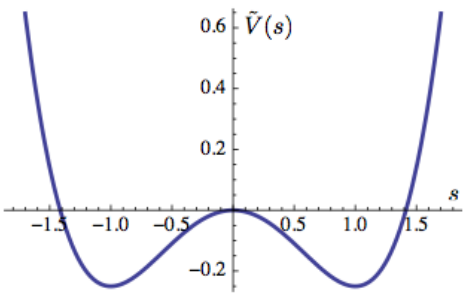

FIG. 2: A graph of the double-well potential. Note the two stable equilibria, shown as valleys and the unstable equilibria shown as a hill. This figure was taken from the unpublished lecture notes of Dr. Nelia Mann.[2]

ergy and still come to rest at the bottom. The unstable equilibrium point in this model would be if the pendulum were standing straight up. If the pendulum is even a little bit off center, then it will return to the stable equilibrium point. The second type of plot used to visualize the motion of the pendulum is the Poincare plot. A Poincare plot has the same axes as the phase space plot, however a point is only plotted once every period of rotation. When an oscillator is moving chaotically, the Poincare plot draws a phenomena called an attractor.[3]

An attractor is an underlying characteristic of chaotic motion. The attractor shows that there are certain points on the phase space plot that seemingly attract points on the Poincare plot. For different systems, there are different attractors. A system's attractor also changes based on the initial conditions. Generally, the basic design of the attractor will not change, but certain aspects of it will be modified. A plot of the potential energy vs. the displacement provides insight into the motion. The potential is found by taking the negative squared velocity. In order to see how a plot of the potential is useful in analyzing the motion of the oscillator, the example of the bistable potential is used. A bistable potential is specific to certain systems, and is another way to describe the motion of system. A bistable potential is commonly called a double-well potential. This comes from the shape of the potential, as shown in Fig. 2. The bistable potential of an oscillator clearly shows where the equilibria are relative to the displacement. These three types of plots provide a decent snapshot of how the oscillator is moving.

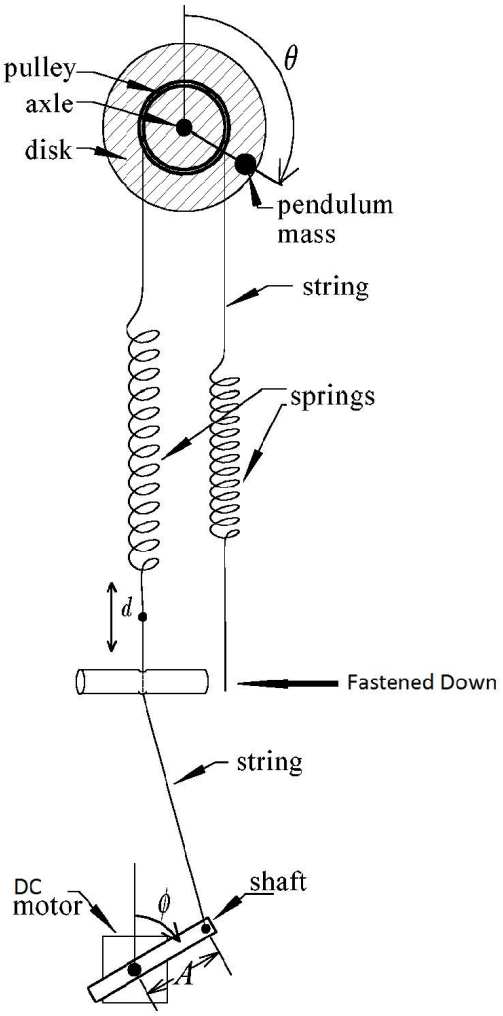

FIG. 3: This is a schematic of the apparatus used to observe and analyze chaotic motion in a mechanical oscillator. Two springs are attached to either side of the pulley. However in the system studied in this experiment, the spring that was tied down, was attached to a secondary vibrational motor. The other spring moves in relation to a rotating rod. The rod is attached to a motor, which is driven by a constant voltage. Not shown are the PASCO Rotary Motion Sensor, PASCO interface box, and voltage source. This figure is taken from Robert DeSerio's work on chaotic pendulums.[4]

II. THEORY

A. Apparatus

This experiment was performed using a mechanical oscillator similar to the one shown in Fig. 3. The only difference was that instead of having one spring tied down, it was attached to a vibrational motor, that oscillated up and down. The rest of the oscillator shown in the figure consisted of a pulley system, with a spring attached to each side. One spring was threaded through a pinhole, and attached to a rotary motor. This motor was controlled by a constant voltage source, ensuring that there would be no acceleration. The other spring was tied off to a fixed point. Doing this ensured that the only force applied to the system would be from the motor. Additionally, a circular disk with a larger radius than the pulley was fixed parallel to the pulley. This disk was aluminum, and had a mass attached to its outer portion. A magnet was placed in close proximity to the disk, providing a damping force.

B. Derivations

Much of this derivation is aided in part by G. Baker[5], N. Mann[2], and S. Kellert.[6]

In order to derive the equation of motion necessary to describe the modified Duffing oscillator, it is useful for clarity's sake to start with a simpler model. Take the simple pendulum described earlier, and as shown in Fig. 1.

The position of the pendulum bob is described by the coordinates (x, y). By writing each coordinate in terms of the angle θ, the position coordinates become

$$\begin{aligned} x &= l\sin\theta \\ y &= -l\cos\theta, \end{aligned} \tag{1}$$

where θ is the angle through which the pendulum swings, as shown in Fig. 1. Using these newly defined coordinates, both the kinetic and potential energies are easily found. The kinetic energy of any object, moving with velocity v, is known to be equal to

$$T = \frac{1}{2}mv^2. \tag{2}$$

From this, it is evident that the velocity of the pendulum bob is needed. The units of velocity is the change in position over the change in time, so a derivative of the position of the object with respect to time yields the velocity of the object. This is written as

$$\begin{aligned} \dot{x} &= l\dot{\theta}\cos\theta \\ \dot{y} &= l\dot{\theta}\sin\theta. \end{aligned} \tag{3}$$

The term $\dot{\theta}$ is the derivative of $\theta(t)$ with respect to time. With this knowledge, the velocity of the pendulum bob is set as

$$\begin{aligned} v^2 &= \left(\dot{x}^2 + \dot{y}^2\right) \\ &= \left(l\dot{\theta}\cos\theta\right)^2 + \left(l\dot{\theta}\sin\theta\right)^2 \\ &= l^2\dot{\theta}^2\left(\cos^2\theta + \sin^2\theta\right) \\ &= l^2\dot{\theta}^2, \end{aligned} \tag{4}$$

where $\dot{x}$ and $\dot{y}$ are the time derivatives of the position of the pendulum bob, as derived earlier. Taking this, and substituting it into Eq. 2, the kinetic energy of the pendulum bob is found. The potential energy of the pendulum bob is simply

$$\begin{aligned} V &= mgy \\ &= -mgl\cos\theta. \end{aligned} \tag{5}$$

Both the kinetic and potential energies derived previously are used to determine the equation of motion of the pendulum. The method of solving for the equation of motion when the total energy of the system is known requires a mathematical function called the Lagrangian. The Lagrangian is defined as the kinetic energy minus the potential energy, and is a way of summarizing the overall dynamics of the system. The Lagrangian of the simple pendulum stated earlier is equal to

$$L = \frac{1}{2}ml^2\dot{\theta}^2 + mgl\cos\theta. \tag{6}$$

In order to derive the equation of motion from the Lagrangian, a differential equation, known as the Euler-Lagrange equation must be found. The Euler-Lagrange equation is as follows,

$$\frac{\partial L}{\partial\theta} = \frac{d}{dt}\left(\frac{\partial L}{\partial\dot{\theta}}\right). \tag{7}$$

In the particular example of the simple pendulum, each derivative is dependent on either θ or $\dot{\theta}$. This particular case has the variable θ in it, however in general, whatever variable changes with respect to time is used. Taking the Euler-Lagrange equation of the Lagrangian in Eq. 6, yields

$$\ddot{\theta} = -\frac{g}{l}\sin\theta. \tag{8}$$

This is the differential equation that describes the equation of motion for the simple pendulum.

C. Applying to the Mechanical Oscillator

Now that the equation of motion for a simple case, like the one outlined earlier, has been derived, these methods are applied to the oscillator in this experiment. Once again, we need to determine the kinetic and potential energies. First, the kinetic energy of the oscillator must be found. While it would be possible to find the kinetic energy by defining x and y coordinates, the math gets more difficult than is necessary. Instead, the kinetic energy of the oscillator is defined in terms of its moment of inertia. This yields

$$T = \frac{1}{2}I\dot{\theta}^2, \tag{9}$$

where I is the moment of inertia.

The potential energy of this oscillator is dependent upon three different components. There are the two spring potentials, which come from each of the springs attached to either side of the oscillator. There is also the gravitational potential energy due to the weighted mass on the edge of the cylindrical disk. First, the potential energy of each spring is calculated to be

$$V_s = \frac{1}{2}k_i d_i^2, \tag{10}$$

where k_i is the spring constant for each of the two springs and d_i is the distance that the spring expands or compresses. The gravitational potential energy due to the mass is equal to

$$V_g = Rmg\left(1 - \cos\theta\right), \tag{11}$$

where R is the radius of the disk attached to the pulley, m is the mass, and g is the acceleration due to gravity. Now, putting all three potential energy terms together, an expression for the total potential energy of the system is given as

$$V_{tot} = \frac{1}{2}k_1 d_1^2 + \frac{1}{2}k_2 d_2 + Rmg\left(1 - \cos\theta\right). \tag{12}$$

While this is an accurate representation of the potential energy, it is not particularly useful experimentally. This is because the distance that the springs stretch, d_i, is dependent on the driving frequencies of each motor. Both of the two motors do essentially the same thing, oscillating at some frequency and amplitude. Because of this, the expressions for both springs take on a similar form. By deriving the first distance, the second can be found with ease.

Looking at the first spring, it is evident that there are two main forces pulling on it. One is due to the driving motor, and the other is due to the tension of the string around the pulley at the apex of the oscillator. In order to determine the total distance the spring is stretched, one of the forces must be held constant, while the other varies. First, the total change in length due to the driving motor is varied, while the change in length due to the pulley is held constant. In order to obtain an expression for the distance the spring expands, the Law of Cosines is used. The resulting equation is written as

$$\Delta d_1 = \sqrt{\left(h + r_o\right)^2 + r_o^2 - 2r_o\left(h + r_o\right)\cos\omega\Delta t} - h, \tag{13}$$

where Δd_1 is the distance the spring expands or compresses, h is the distance that the motor displaces the string. As is evident from this equation, the potential energy of the spring will be dependent upon the driving frequency ω.

Through some algebraic manipulations as well as simplification, the equation outlined is written as

$$\Delta d_1 = h\left[\sqrt{\left(1 + \frac{r_o}{h}\right)^2 + \frac{r_o^2}{h^2} - 2\frac{r_o}{h}\left(1 + \frac{r_o}{h}\right)\cos\omega\Delta t} - 1\right]. \tag{14}$$

With this new expression, setting $r_o << h$ allows for most of the terms to go to zero. This assumption is allowed, because the amplitude of the driving force is much less than the length of the string. Doing this yields the equation

$$\Delta d_1 = r_o\left(1 - \cos\omega\Delta t\right). \tag{15}$$

In order to get the full picture of the forces acting on the spring, distance that the spring changes due to the pulley is needed. This is much easier to derive than the previous derivation. Taking into account that there is little to no slippage of the string on the pulley, the amount the string moves is equal to

$$\Delta d_1 = -r_p\Delta\theta. \tag{16}$$

It is important to note that r_p is the radius of the pulley and not the driving amplitude.

In order to obtain the net change in the spring, the two terms must be summed. The reason that the terms can simply be summed is that when the string is pulled in one direction due to the driving motor, the pulley will follow suit. Doing this, the net change in the length of the spring is equal to

$$d_1 = d_o + r_o\left(1 - \cos\omega t\right) - r\theta. \tag{17}$$

The term d_o is added to the end of the equation as a correction factor due to the fact that the spring does not start from its equilibrium point each time.

Taking the methods used to define the displacement of the first spring and drawing from it, we can get

$$d_2 = d_o + s\left(1 - \cos\tilde{\omega}t\right) + r_p\theta, \tag{18}$$

where s is the amplitude of the second motor, and $\tilde{\omega}$ is the frequency of the second motor. This looks very similar to Eq. 17, as it should due to the symmetry of the system. Both of the equations for the displacement of each spring are substituted into the total potential energy equation, Eq. 12. This provides an equation for the total potential energy in terms of easily measurable quantities. Finding the Euler-Lagrange equations using this newly derived potential energy, the equation of motion is found to be

$$I\ddot{\theta} = -mgR\sin\theta - 2kr_p^2\theta + r_p ks\cos\tilde{\omega}t - r_p kr_o\cos\omega t. \tag{19}$$

This equation describes the motion of the oscillator as it rotates.

III. PROCEDURE

The analysis of the modified Duffing oscillator required some adjustments to be made to the original Duffing oscillator. The original Duffing oscillator consisted of a pulley with string wrapped around it, and two springs coming off of each side, as shown in Fig. 3. One of the springs was attached to a driving motor, while the other was tied down. The driving motor was a rotational motor, with variable frequency and amplitude. Once every period, the driving motor would pass through a photogate and record the position of the oscillator. A damping magnet was attached behind the aluminum disk. The distance between the damping magnet and the aluminum disk was variable. Finally, the initial position of the point mass on the pulley was movable. Each of these conditions had been studied previously in lab, so in order to analyze the chaotic motion of the oscillator, some changes were made.

In order to modify the oscillator, the spring that was fastened down was attached to a vibrational motor. The vibrational motor moved the string up and down by a total of 1 cm. The frequency with which the motor oscillated was variable, ranging from 0 Hz to 3 Hz. In

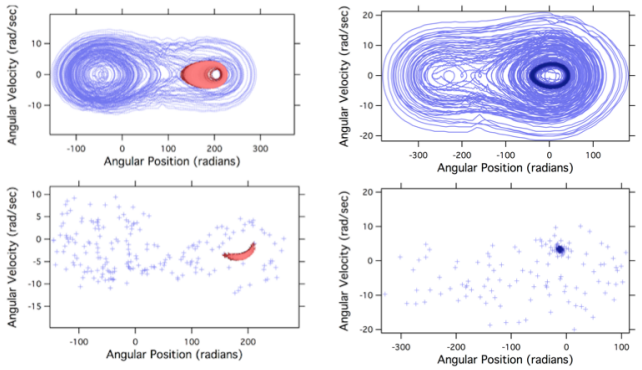

FIG. 4: Phase space and Poincare plot comparison for the apparatus, with one spring fixed (left), and also the same apparatus with the spring vibrating (right). This slight change must have been enough to vary the motion of the oscillator.

order make the modified oscillator similar to the original oscillator, the entire oscillator was raised off of the table so that the vibrational motor sat at approximately where the spring was tied off. The vibrational motor was attached to a function generator, and attached up to an oscilloscope. The oscilloscope provided a way to view the voltage of the second motor, while the function generator provided the frequency of oscillation. A Pasco box was set up with a computer, and had inputs coming from the motor, rotary wheel, and photogate. When the motor was set to the off position, a clamp was placed around it so that there would be no additional movement due to string tension. The effect of the second motor on the motion of the oscillator was recorded in two different plots. The first plot, the phase space plot, was used to observe the change in angle vs the change in frequency, or $\{\theta, \omega\}$. The other plot that was used was the Poincare plot, which had the same parameters as the phase space plot, however a point is recorded once every period.

IV. RESULTS AND ANALYSIS

In order to see how the modifications changed the motion of the oscillator, the second motor was turned off and clamped. The voltage of the first motor was set to one of the voltages observed in previous runs. The original motor was then turned on, and data was collected for an hour. This was then compared to the mentioned previous data set, as shown in Fig. 4. For the most part, the phase space diagrams will be left out of the report, as the differences in them are quite subtle. The Poincare plots show the differences in motion much more clearly.

Once a baseline was established, the damping magnet was looked at. At first, it seemed like a good idea to detach the magnet entirely. This is due to the fact that the damping magnet merely slowed the oscillators movement, and made the motion periodic. The magnet was ultimately left on the oscillator, as it is controllable. The

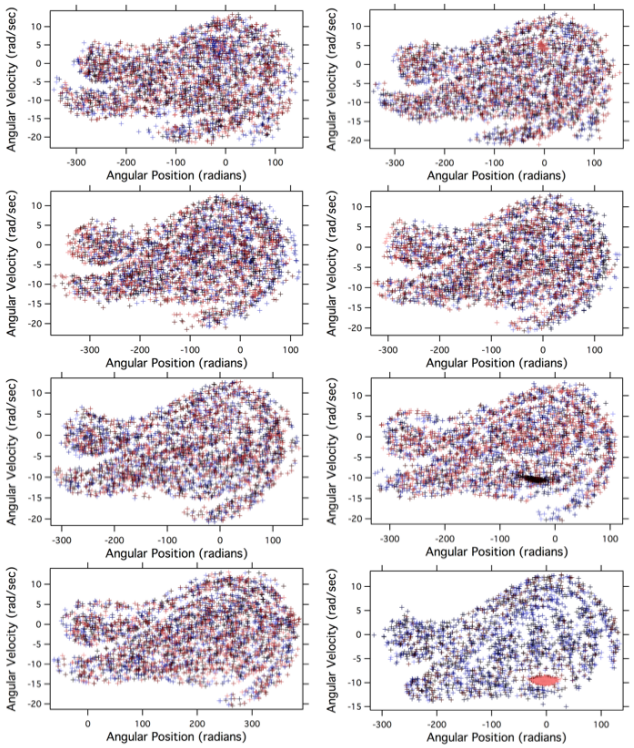

FIG. 5: Poincare plots for varying frequency of vibration. The frequency of the motor was increased as the plots go from top left to bottom right. As is evident from these graphs, there is a patterned shift in the plots. This patterned shift clearly shows how the Poincare plot changes over time. The voltage of the rotary motor was held constant at 6.05 V, while the frequency of the vibrational motor was varied from 0.00 Hz to 3.00 Hz.

friction of the pulley is nearly impossible to measure in this case and will not be uniform over the entire surface of the pulley. The damping magnet's use in this case is that of minimizing the effect of friction. The damping magnet's force is so much greater than the force due to friction, that the effect of friction essentially goes to zero.[7]

The next step was to increase the frequency of the additional motor, while holding the original motor constant. After taking the first data run with the second motor on, an immediate change was seen. The motion of the oscillator changed from periodic to chaotic. This clearly shows that the additional motor did indeed affect the motion of the oscillator. It makes sense that there would be a change in motion, because chaotic motion is extremely sensitive to changes in initial conditions. The original motor was held at 6.05 V, while the frequency of the second was increased in fairly similar intervals. As the frequency of the additional motor increased, the Poincare plot slowly began to shift. This can be seen in Fig. 5.

The gradual change in the attractor pictured is much different than the changes that occurred in attractors,

when just one motor was active. The results from previous trials showed that there seemed to be no easily seen correlation between increasing the frequency of the motor. This new insight is interesting, because rough predictions of how the oscillator will move can be made. Now while the predictions will be very primitive and limited to the Poincare plot, there is some level of order to the system. Long term accurate predictions are still impossible to create, as is the case for all chaotic systems. Comparing both the previous Poincare plots to the new Poincare plots, the difference between the two is clear. While they look drastically different from each other, there are some underlying similarities. It seems as though the left side of the plot shrunk once the additional motor was added, while the right side of the plot seemed to grow. These similarities are due to the fact that the oscillator is still very similar to the Duffing oscillator, so it makes sense that the motion would at the very least be similar. In order to determine if it the correlation was due to the addition of a second motor, or if it was simply due to how the vibrational motor worked, the frequency of the rotary motor was varied while the frequency of the vibrational motor was held constant. The resulting Poincare plots did not show a clear correlation like the vibrational motor did. This means that the reason for the correlation was due to the technicalities of the vibrational motor. One reason that this would happen is that the vibrational motor moves such a small distance, that a change in the frequency of the motor would have very little effect on the overall motion of the system. It would, however, have just enough of an effect to alter the Poincare plot.

The fact that attaching the vibrational motor to the oscillator immediately changed the Poincare plot, prompted some observations into how the angle of the spring affects motion. The angle of the spring was changed three different times, and data was taken for each. The resulting Poincare plots show that changing the angle of the spring has a noticeable effect on the motion of the oscillator. The change in the motion of the oscillator due to varying angles is shown in Fig. 6. The fact that the angle that the spring is at changes how the system behaves is an important fact. This means that the derivation from earlier is not going to be exact. The derivation assumes that both springs are hanging straight down, whereas in reality neither of them are vertical. The initial starting point for the mass was not changed due to the high variability of starting angles. It would have been near impossible to ensure accurate drop locations for each run. There are also endless possibilities for starting angles.

Finally, the derivation from earlier was used to attempt to simulate one of these data runs. In order to simulate the system, Mathematica was used. The equation of motion was entered into Mathematica's NDSolve function, however due to the numerous constants, no result was obtained. To remedy this, all of the measurable constants were found, and substituted into the equation of motion

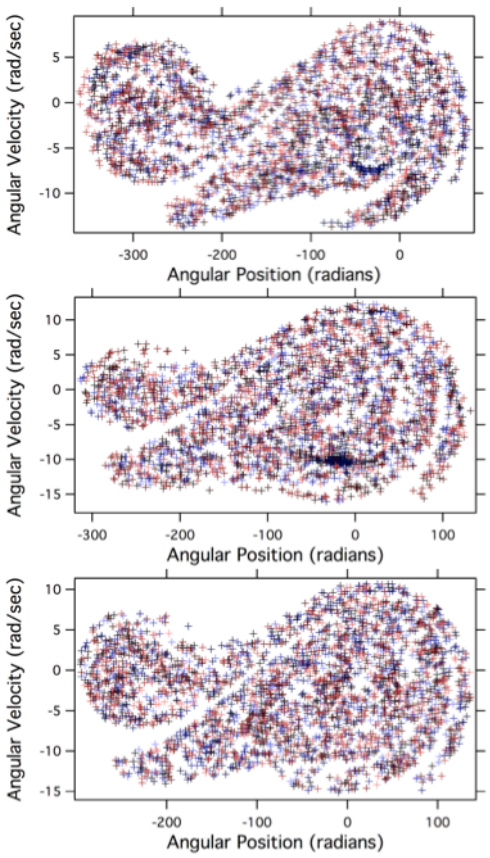

FIG. 6: This figure shows the different Poincare plots for varying spring angles. The second graph in this figure looks very similar to some of the graphs observed from the original Duffing oscillator. This variance in plots is due to both the changing angle as well as the different tensions put on the spring. There is no real correlation or pattern between the angles, however with such a small sample size it is impossible to draw any in depth conclusions. The plots are read from top to bottom, and are placed in order of increasing angle.

so that there were constants of only the angle of rotation, θ, and the elapsed time, t. Doing this left a second order differential equation, that was fairly easy for Mathematica to solve. The resulting phase space diagram is shown in Fig. 7. From this, it is evident that the phase space diagram is does not exactly match up with the one shown in Fig. 4. What can be drawn from the theoretical phase space diagram is that the general shape of the phase space is the same, so we are at least on the right track. The phase plot also shows that the system unpredictably oscillates between the two equilibrium points

A. Error Analysis

In this experiment, there were several sources for error. First, as stated earlier, the springs were not exactly vertical. This meant that the system could not be modeled perfectly. The springs were also assumed to be the

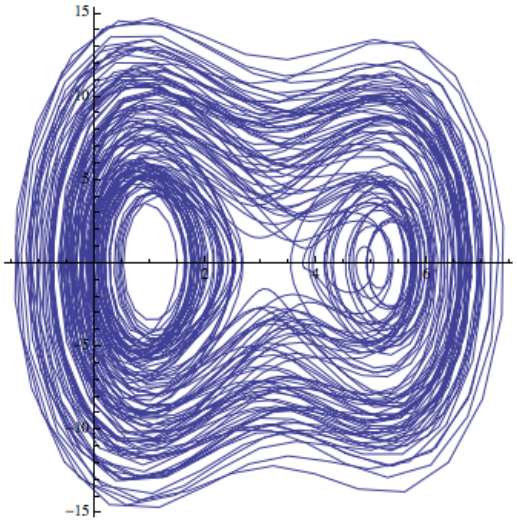

FIG. 7: This is a theoretical phase space plot based upon the equation of motion derived in the Theory. It is not completely accurate due to assumptions that had to be made, but nonetheless it is still useful as a rough guide for the phase space.

exact same, which they were not, as it is experimentally impossible to ensure both springs are perfectly symmetrical. This would have skewed the experimental values found for the spring constant, as only one was measured. Another source of error was the fact that the vibrational motor was not a precise tool. While the motor was running, the oscillations were not smooth. As the motor moved up and down, there were slight vibrations that were not in line with the smooth oscillations assumed. The motor also moved the spring further away from being vertical. Had there been more time, a hole could have been cut into the platform, and the vibrational motor placed under the hole, so as to minimize the angle off of the vertical. Another cause of error was the fact that both the voltage source and the function generator were not very accurate. When hooking a voltmeter up to the voltage source, fluctuations in voltage were common, thus skewing the results. The function generator was also not entirely accurate, however there was not a great way to numerically determine how off it actually was.

V. CONCLUSION

This lab allowed for further analysis of the Duffing oscillator with an additional motor. It was found that the additional motor caused some interesting behavior in the oscillator. When the frequency of the additional motor was increased, the Poincare plot seemed to morph into a new plot. Had there been more precise tools, a time-lapse of the Poincare plot could have been developed for each frequency. Despite this, we also found that the angle of the spring changes the motion of the oscillator. This was interesting because even in the original Duffing oscillator, there was some angle off the vertical as well. Finally, it was discovered that changing the amplitude of either of the motors reacted in the same way as in the original Duffing oscillator. There was seemingly no pattern as to why or when the motion would change. One thing is for sure, the motion of the oscillator is extremely sensitive to initial conditions.

[1] Davies, Brian; *Exploring Chaos: theory and experiment* Perseus Books (1999).

[2] Dr. Nelia Mann, *Unpublished Lecture Notes* (2015).

[3] J.B., *Classical Dynamics*, Academic Press Inc. University of Maryland, College Park. p.203-211 (1970).

[4] Robert Deserio, *Chaotic Pendulum: The Complete Attractor*, American Journal of Physics. 71, 250-257 (2003).

[5] Gregory L. Baker; James A. Blackburn *The Pendulum: a case study in physics*, Oxford University Press (2006).

[6] Stephen H. Kellert, *In the Wake of Chaos, Unpredictable Order in Dynamical Systems.*, University of Chicago Press (1993).

[7] Martell, E.C.; Martell, V.B.; *The Effect of Friction in Pulleys on the Tension in Cables and Strings.* Physics Teacher, vol 51, no 2 (2013).

[8] Tufillaro, N.B.; Abbot, T.; Reilly, J.; *An Experimental Approach to Nonlinear Dynamics and Chaos* Addison-Wesley Publishing Co (1992).

[9] Smith Jr., B.R.; *The Quadratically Damped Oscillator: A case study of a non-linear equation of motion.* American Journal of Physics (2012).